International Telecommunication Union

ITU-R

Radiocommunication Sector of ITU

**Recommendation ITU-R M.1851-1**
**(01/2018)**

# Mathematical models for radiodetermination radar systems antenna patterns for use in interference analyses

**M Series**

**Mobile, radiodetermination, amateur and related satellite services**

## Foreword

The role of the Radiocommunication Sector is to ensure the rational, equitable, efficient and economical use of the radio-frequency spectrum by all radiocommunication services, including satellite services, and carry out studies without limit of frequency range on the basis of which Recommendations are adopted.

The regulatory and policy functions of the Radiocommunication Sector are performed by World and Regional Radiocommunication Conferences and Radiocommunication Assemblies supported by Study Groups.

## Policy on Intellectual Property Right (IPR)

ITU-R policy on IPR is described in the Common Patent Policy for ITU-T/ITU-R/ISO/IEC referenced in Annex 1 of Resolution ITU-R 1. Forms to be used for the submission of patent statements and licensing declarations by patent holders are available from http://www.itu.int/ITU-R/go/patents/en where the Guidelines for Implementation of the Common Patent Policy for ITU-T/ITU-R/ISO/IEC and the ITU-R patent information database can also be found.

### Series of ITU-R Recommendations

(Also available online at **http://www.itu.int/publ/R-REC/en**)

| Series | Title |
|---|---|
| **BO** | Satellite delivery |
| **BR** | Recording for production, archival and play-out; film for television |
| **BS** | Broadcasting service (sound) |
| **BT** | Broadcasting service (television) |
| **F** | Fixed service |
| **M** | **Mobile, radiodetermination, amateur and related satellite services** |
| **P** | Radiowave propagation |
| **RA** | Radio astronomy |
| **RS** | Remote sensing systems |
| **S** | Fixed-satellite service |
| **SA** | Space applications and meteorology |
| **SF** | Frequency sharing and coordination between fixed-satellite and fixed service systems |
| **SM** | Spectrum management |
| **SNG** | Satellite news gathering |
| **TF** | Time signals and frequency standards emissions |
| **V** | Vocabulary and related subjects |

***Note***: *This ITU-R Recommendation was approved in English under the procedure detailed in Resolution ITU-R 1.*

*Electronic Publication*
Geneva, 2018

RECOMMENDATION ITU-R M.1851-1

# Mathematical models for radiodetermination radar systems antenna patterns for use in interference analyses

(2009-2018)

**Scope**

This Recommendation describes radiodetermination radar systems antenna patterns to be used for single-entry and aggregate interference analysis. Dependent on the antenna 3 dB beamwidth and first peak side-lobe level, the proper set of equations for both azimuth and elevation patterns may be selected. Both peak, for single interferer, and average patterns, for multiple interferers, are defined.

**Keywords**

Antenna patterns, current distribution, illumination field, peak and average mask pattern equations

**Abbreviations/Glossary**

ADP Antenna directivity pattern

**Related ITU-R Recommendations**

Recommendations ITU-R F.699, ITU-R F.1245, ITU-R M.1638, ITU-R M.1652, ITU-R M.1849

The ITU Radiocommunication Assembly,

*considering*

that a mathematical model is required for generalized patterns of antennas for interference analyses when no specific pattern is available for the radiodetermination radar systems,

*recommends*

**1** that, if antenna patterns and/or pattern equations applicable to a radar(s) are available in other ITU-R Recommendations dealing with radiodetermination radar system characteristics, then those should be used;

**2** that, in the absence of information concerning the antenna patterns of the radiodetermination radar system antenna involved, one of the mathematical reference antenna models described in Annex 1 should be used for interference analysis.

# Annex 1

# Mathematical models for radiodetermination radar systems antenna patterns for use in interference analyses

## 1 Introduction

A generalized mathematical model for radiodetermination radar systems antenna patterns is required when these patterns are not defined in ITU-R Recommendations applicable to the radiodetermination radar system under analysis. Generalized antenna pattern models could be used in analyses involving single and multiple interferer entries, such as that from other radar and communication systems.

This text describes proposed antenna patterns to be used. Given knowledge about beamwidth and the first peak side-lobe level, the proper set of equations for both azimuth and elevation patterns may be selected.

The result of surveyed antenna parameter ranges from ITU-R Recommendations are recorded in Table 1.

TABLE 1

**Surveyed antenna parameter limits**

| Antenna parameter | Units | Description | Minimum value | Maximum value |
|---|---|---|---|---|
| Transmit and receive frequencies | MHz | | 420 | 33 400 |
| Antenna polarization type | | Horizontal, vertical, circular | | |
| Antenna type | | Omni, yagi element array, parabolic reflector, phased array | | |
| Beam type – most common | | Fan, pencil, cosecant squared | | |
| Transmit and receive gain | dBi | | 25.6 | 54 |
| Elevation beamwidth (–3dB) | degrees | Pencil beam | 0.25 | 5.75 |
| | | Cosecant squared ($CSC^2$) (equation (12) and Table 4) | 3.6 ($\theta_3$)<br>20 ($\theta_{Max}$) | 3.6 ($\theta_3$)<br>44 ($\theta_{Max}$) |
| Azimuth beamwidth (–3dB) | degrees | Pencil beam | 0.4 | 5.75 |
| Elevation scan angle limit | degrees | | –60 | +90 |
| Azimuth scan angle limit | degrees | | 30 sector | 360 |
| First side-lobe level below main lobe peak | dB | | –35 | –15.6 |

Table 1 was used to guide the development of the antenna types and patterns proposed.

## 2 Mathematical formulae

### 2.1 Radar antenna with a narrow beamwidth

#### 2.1.1 Background

In the absence of neither particular information concerning the 3 dB beamwidth or the shape of the current distribution or illumination field on the antenna aperture, but in the presence of information given about the size of the antenna, the $\theta_3$ half power beam-width (degrees) is approximated by $70\,\lambda/D$, where $\lambda$ the wavelength and D the antenna length are expressed in the same units; see Recommendation ITU-R F.699, *recommends* 4.1.

If the information about the shape of the current distribution or illumination field on the antenna aperture is accessible, then a more accurate model of the antenna pattern can be used.

To simplify the analysis, the antenna current distribution is considered as a function of either the elevation or azimuth coordinates. The directivity pattern, $F(\mu)$, of a given distribution is found from the finite Fourier transform as:

$$F(\mu) = \frac{1}{2}\int_{-1}^{+1} f(x)\cdot e^{j\mu x}\,dx \qquad (1)$$

where:

$f(x)$: relative shape of field distribution, see Table 2 and Fig. 1

$\mu$: provided in the table below = $\pi\left(\frac{l}{\lambda}\right)\sin(\alpha)$

$l$: overall length of aperture

$\lambda$: wavelength

$\omega$: beam elevation or azimuth pointing (scan) angle relative to aperture normal

$\theta$: point of interest direction angle relative to aperture normal

$\alpha$: point of interest direction angle relative to pointing angle direction ($\alpha=\theta-\omega$)

$x$: normalized distance along aperture $-1 \le x \le 1$

$j$: complex number notation.

FIGURE 1

**Antenna polar diagram mask**

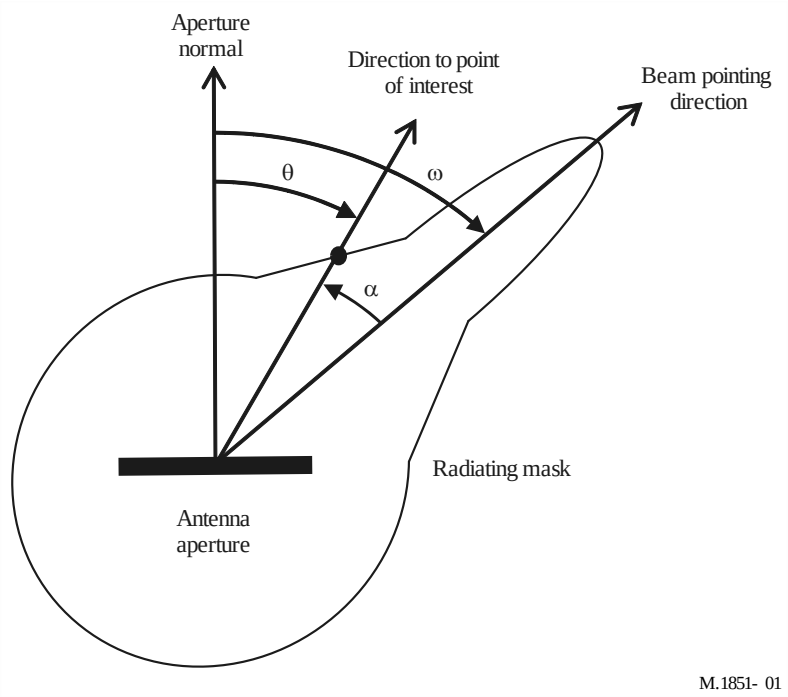


The proposed theoretical antenna patterns for antennas having uniform phase field distribution are provided in Table 2.

The proposed theoretical antenna patterns for phased array antennas are given in § 7, taking into account specific sidelobes effects arising at large scan ω angles.

The parameters and formulae for determining antenna directivity patterns (ADP) that are presented in Table 2 (and thereafter in the related Table 3 and Figures) are correct only in the case where the field amplitude at the edge of the antenna aperture is equal to zero and within the bounds of the main lobe and first two side lobes of the ADP.

With other values of field amplitude at the edge of the antenna aperture, the form of the ADP and its parameters may differ significantly from the theoretical ones presented in this Recommendation.

In absence of any other information, a simplified antenna pattern fitting with the theoretical main lobe and a mask in other directions may be considered for sharing and compatibility studies with radar systems. Peak or average masks are recommended for doing such studies with respectively single or multiple interferers. The mask departs at break point issued from theoretical pattern and decreases over sidelobes down to a floor mask to represent antenna far side lobes and back lobes, as described in § 2.1.3.

If real radar antenna patterns are available, then those should be digitized and used.

### 2.1.2 Theoretical antenna equations

Equations of directivity patterns and associated parameters are given in Table 2 for different shape of field distribution on the antenna aperture.

TABLE 2

**Theoretical antenna directivity parameters**

| **Relative shape of field distribution $f(x)$ where $-1 \le x \le 1$** | **Directivity pattern $F(\mu)$** | **$\theta_3$ half power beam-width (degrees)** | **$\mu$ as a function of $\theta_3$** | **First side-lobe level below main lobe peak (dB)** | **Equation No.** |
|---|---|---|---|---|---|
| Uniform value of 1 | $\frac{\sin(\mu)}{\mu}$ | $50.8\left(\frac{\lambda}{l}\right)$ | $\frac{\pi \cdot 50.8 \cdot \sin(\theta)}{\theta_3}$ | −13.2 | (2) |
| COS($\pi$*$x$/2) | $\frac{\pi}{2}\left[\frac{\cos(\mu)}{\left(\frac{\pi}{2}\right)^2 - \mu^2}\right]$ | $68.8\left(\frac{\lambda}{l}\right)$ | $\frac{\pi \cdot 68.8 \cdot \sin(\theta)}{\theta_3}$ | −23 | (3) |
| COS $^2$($\pi$*$x$/2) | $\frac{\pi^2}{2 \cdot \mu}\left[\frac{\sin(\mu)}{\left(\pi^2 - \mu^2\right)}\right]$ | $83.2\left(\frac{\lambda}{l}\right)$ | $\frac{\pi \cdot 83.2 \cdot \sin(\theta)}{\theta_3}$ | −32 | (4) |
| COS $^3$($\pi$*$x$/2) | $\frac{3 \cdot \pi \cdot \cos(\mu)}{8}\left[\frac{1}{\left(\frac{\pi}{2}\right)^2 - \mu^2} - \frac{1}{\left(\frac{3 \cdot \pi}{2}\right)^2 - \mu^2}\right]$ | $95\left(\frac{\lambda}{l}\right)$ | $\frac{\pi \cdot 95 \cdot \sin(\theta)}{\theta_3}$ | −40 | (5) |
| COS$^4$($\pi$*$x$/2) | $\frac{3\pi^4 \sin(\mu)}{2\mu\left(\mu^2 - \pi^2\right)\left(\mu^2 - 4\pi^2\right)}$ | $106\left(\frac{\lambda}{l}\right)$ | $\frac{\pi \cdot 106 \cdot \sin(\theta)}{\theta_3}$ | −47 | (6) |

where $\theta_3$ is the 3 dB antenna half-power beamwidth (degrees). The relative shapes of the field distribution functions $f(x)$, as defined in Table 2, are plotted in Fig. 2.

FIGURE 2

**Aperture distributions**

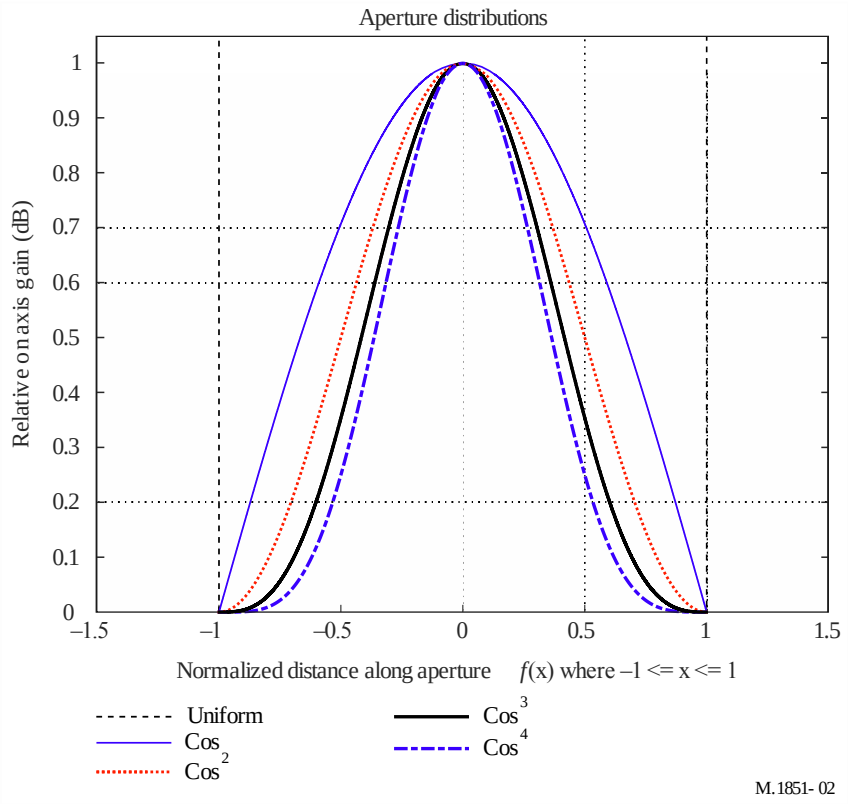


Given that the half power beamwidth, $\theta_3$, is provided, the value of $\mu$ can be redefined as a function of the half-power antenna beamwidth. This is done by replacing the quantity $\left(\frac{l}{\lambda}\right)$ in $\mu = \pi\left(\frac{l}{\lambda}\right)\sin(\theta)$ by a constant that depends on the relative shape of the field distribution; divided by the half-power beamwidth, $\theta_3$, as shown in Table 2. These constant values of 50.8, 68.8, 83.2, 95 and 106, shown in Table 2, can be derived by setting the equation for $F(\mu)$ equal to −3 dB, and solving for the angle $\theta$.

Figure 3 shows various linear aperture antenna patterns for uniform, cosine (COS), cosine-squared ($COS^2$) and cosine-cubed ($COS^3$) and cosine-to-the-fourth power ($COS^4$) field distribution functions. As the patterns are mathematically symmetric, they have been partially traced on the diagram. For comparison, all patterns are set to a same 3 dB beamwidth of 6.0 degrees, meaning different ratios for $\lambda/l$.

FIGURE 3

**Antenna pattern comparison for various linear aperture distributions, 3 dB beamwidth is 6.0 degrees (pattern is symmetric)**

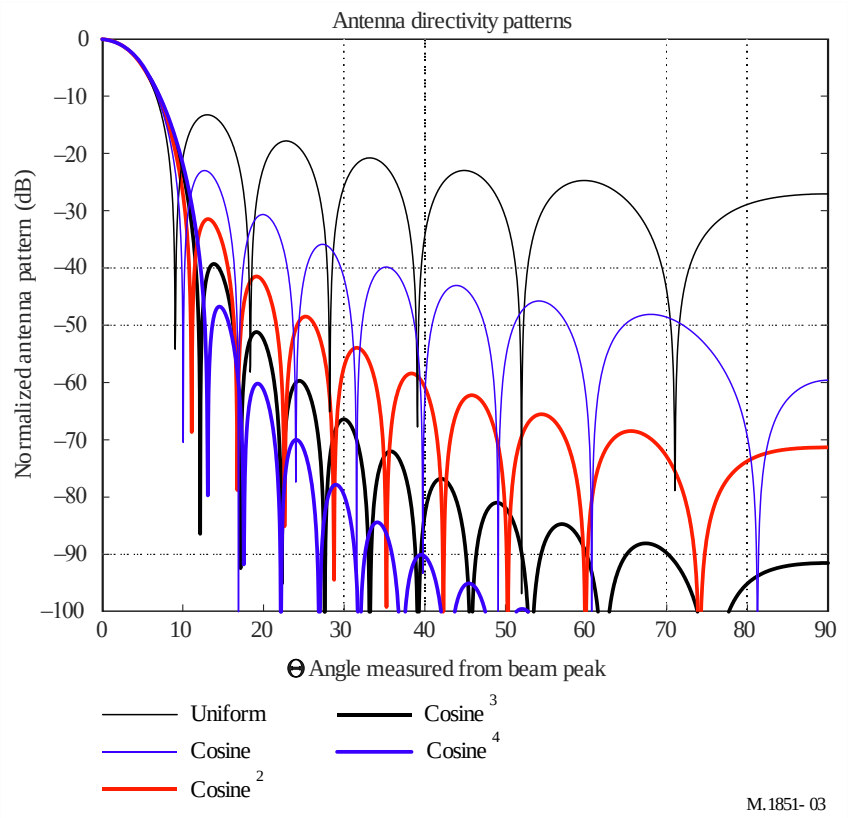


### 2.1.3 Procedure for mask determination

Using Fig. 3 above, the mask equations are derived by using a curve fit to the antenna peak side-lobe levels. It has been found, by comparing the integral of the theoretical and the proposed mask patterns, that the difference between the peak and average power in one principal plane cut is approximately 4 dB. The following definitions apply:

– convert equations (2) to (6) into dB using $20*\log_{10}$ (absolute value (field directivity pattern));

– normalize the antenna pattern gains. Uniform field distribution does not require normalization, for cosine one subtract −3.92 dB, for cosine-squared one subtract −6.02 dB and for cosine-cubed one subtract −7.44 dB, and for cosine-to-the-fourth power one subtract −8.52 dB;

– to plot the mask, use the theoretical directivity pattern from Table 2, as shown in the previous two steps, up to the break point for either the peak or average antenna pattern, as required. After the break point, apply the mask pattern as indicated in Table 3;

– the peak pattern mask is the antenna pattern that rides over the side-lobe peaks. It is used for a single-entry interferer;

– the average pattern mask is the antenna pattern that approximates the integral value of the theoretical pattern. It is used for aggregated multiple interferers;

– the peak pattern mask break point is the point in pattern magnitude (dB) below the maximum gain where the pattern shape departs from the theoretical pattern into the peak mask pattern, as shown in Table 3;

– the average pattern mask break point is the point in pattern magnitude (dB) below the maximum gain where the pattern shape departs from the theoretical pattern into the average mask pattern, as shown in Table 3;

– $\theta_3$ is the 3 dB antenna beamwidth (degrees);

– $\theta$ is the angle in either the elevation (vertical) or azimuth (horizontal) principal plane cuts (degrees);

– the average mask is the peak mask minus approximately 4 dB. Note that the break points of the peak pattern are different from the average patterns.

Table 3 shows the equations to be used in the calculations.

TABLE 3

**Peak and average theoretical mask pattern equations**

| **Field distribution** | **Mask equation beyond pattern break point where mask departs from theoretical pattern (dB)** | **Peak pattern break point where mask departs from theoretical pattern (dB)** | **Average pattern break point where mask departs from theoretical pattern (dB)** | **Constant added to the peak pattern to convert it to average mask (dB)** | **Mask floor level (dB)** | **Equation No.** |
|---|---|---|---|---|---|---|
| Uniform | $-8.584 \cdot \ln\left(2.876 \cdot \frac{\lvert\theta\rvert}{\theta_3}\right)$ | −5.75 | −12.16 | −3.72 | −30 | (7) |
| COS | $-17.51 \cdot \ln\left(2.33 \cdot \frac{\lvert\theta\rvert}{\theta_3}\right)$ | −14.4 | −20.6 | −4.32 | −50 | (8) |
| $COS^2$ | $-26.882 \cdot \ln\left(1.962 \cdot \frac{\lvert\theta\rvert}{\theta_3}\right)$ | −22.3 | −29.0 | −4.6 | −60 | (9) |
| $COS^3$ | $-35.84 \cdot \ln\left(1.756 \cdot \frac{\lvert\theta\rvert}{\theta_3}\right)$ | −31.5 | −37.6 | −4.2 | −70 | (10) |
| $COS^4$ | $-45.88 \cdot \ln\left(1.56 \cdot \frac{\lvert\theta\rvert}{\theta_3}\right)$ | −39.4 | −42.5 | −2.61 | −80 | (11) |

The function ln() is the natural logarithm function. An example of the break point is shown in Fig. 4.

FIGURE 4

**Break point example**

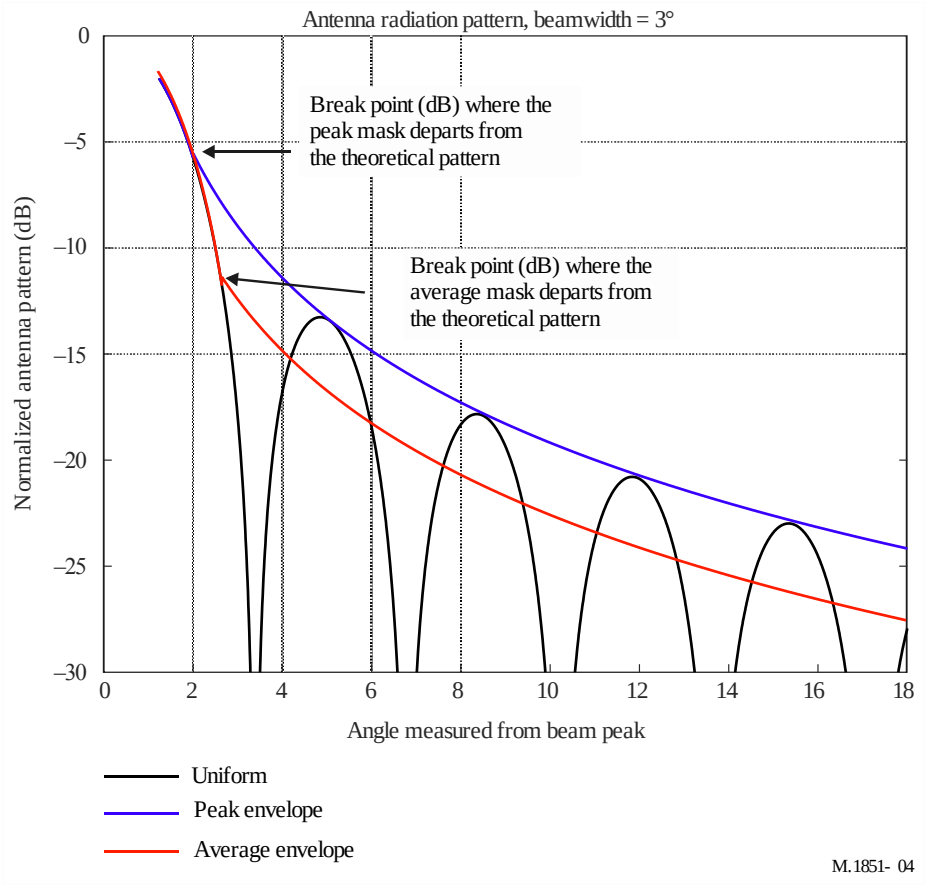


## 2.2 Radar antenna with a cosecant-squared elevation pattern

The cosecant-squared pattern is a special case. The power (not field-strength) is given by:

$$G(\theta) = G(\theta_1) \cdot \left( \frac{CSC(\theta)}{CSC(\theta_1)} \right)^2 \quad (12)$$

where:

$G(\theta)$: cosecant squared pattern between angles of $\theta_1$ and $\theta_{Max}$

$G(\theta_1)$: pattern gain at $\theta_1$

$\theta_1$: half power antenna beamwidth where cosecant-squared pattern starts = $\theta_3$

$\theta_{Max}$: maximum angle where cosecant-squared pattern stops

$\theta$: elevation angle (degrees)

$\theta_3$: half power antenna beamwidth (degrees).

The average antenna pattern gain is not considered for the cosecant-squared pattern. It should be used for single and multiple interferers. The cosecant pattern is applied as shown in Table 4:

TABLE 4

**Cosecant-squared antenna pattern equations**

| Cosecant-squared equation | Condition | Equation No. |
|---|---|---|
| $\frac{\sin(\mu)}{\mu};\ \mu = (\pi \cdot 50.8 \cdot \sin(\theta))/\theta_3$ | $\frac{-\theta_3}{0.88} \le \theta \le +\theta_3$ | (13) |
| $G(\theta_1) \cdot \left( \frac{CSC(\theta)}{CSC(\theta_1)} \right)^2$ | $+\theta_3 \le \theta \le \theta_{Max}$ | (14) |
| Cosecant floor level (example = −55 dB) | $\theta_{Max} \le \theta \le \theta_{90}$ | (15) |
| $G(\theta_1) = \frac{\sin\left( \frac{\pi \cdot 50.8 \cdot \sin(\theta_1)}{\theta_3} \right)}{\frac{\pi \cdot 50.8 \cdot \sin(\theta_1)}{\theta_3}}$ | $\theta_1 = \theta_3$ | (16) |

*Note that* $G(\theta_1) \cdot \left( \frac{CSC(\theta)}{CSC(\theta_1)} \right)^2$ refers to the amplitude of the power pattern, while $\frac{\sin(\mu)}{\mu}$ and $G(\theta_1) = \frac{\sin\left( \frac{\pi \cdot 50.8 \cdot \sin(\theta_1)}{\theta_3} \right)}{\frac{\pi \cdot 50.8 \cdot \sin(\theta_1)}{\theta_3}}$ refer to the 'Directivity pattern F(μ)', field amplitude; which are square of power amplitude. The solution might be writing $\left( \frac{\sin(\mu)}{\mu} \right)^2$ and $G(\theta_1) = \left( \frac{\sin\left( \frac{\pi \cdot 50.8 \cdot \sin(\theta_1)}{\theta_3} \right)}{\frac{\pi \cdot 50.8 \cdot \sin(\theta_1)}{\theta_3}} \right)^2$

A graphical description of the patterns is shown in the Figures below.

FIGURE 5

**Cosecant squared beam coverage for search radar**

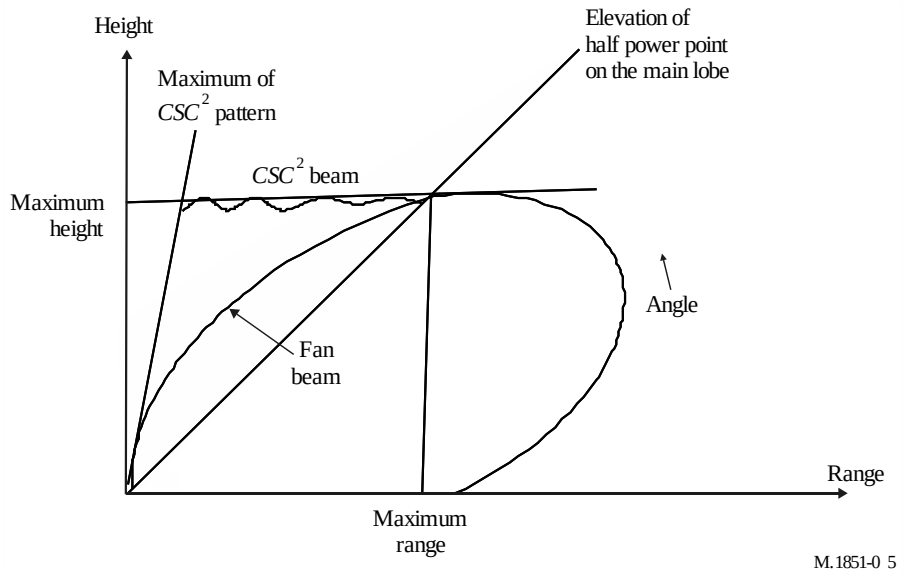

## 2.3 Theoretical diagrams and masks for different antenna radiation patterns

FIGURE 6

**Antenna pattern, peak $\left(\frac{\sin\theta}{\theta}\right)^2$ in radians or $\left(\frac{\sin\theta}{\theta}\times\frac{180}{\pi}\right)^2 \approx \left(\frac{\sin\theta}{\theta}\times 57.3\right)^2$ in degrees, and average envelope for uniform field distribution**

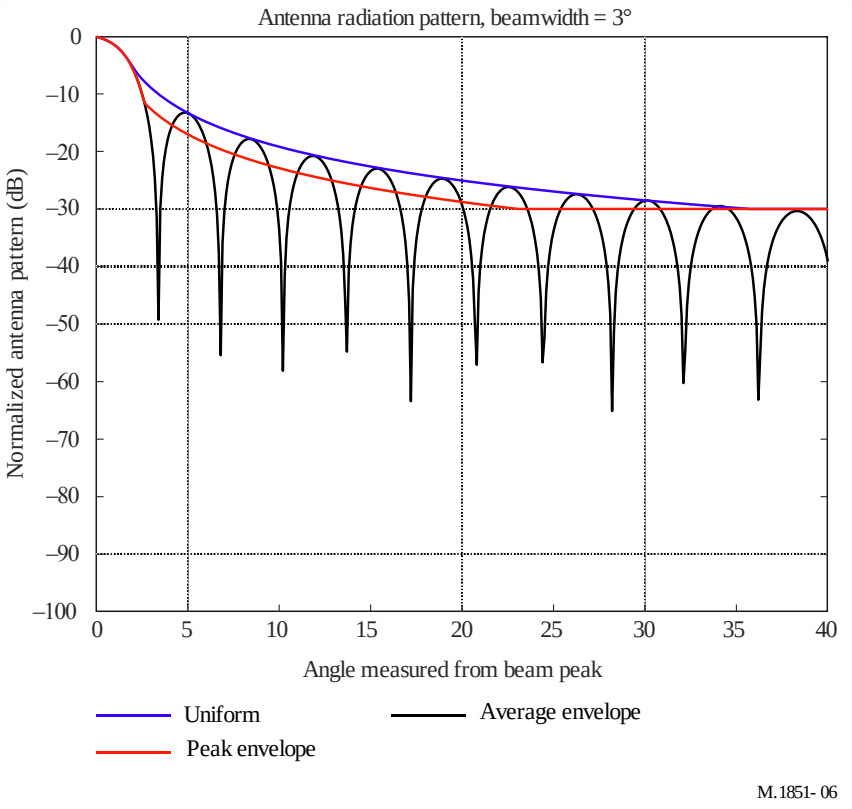

FIGURE 7

**Example polar plot antenna pattern, peak and average envelope for uniform field distribution**

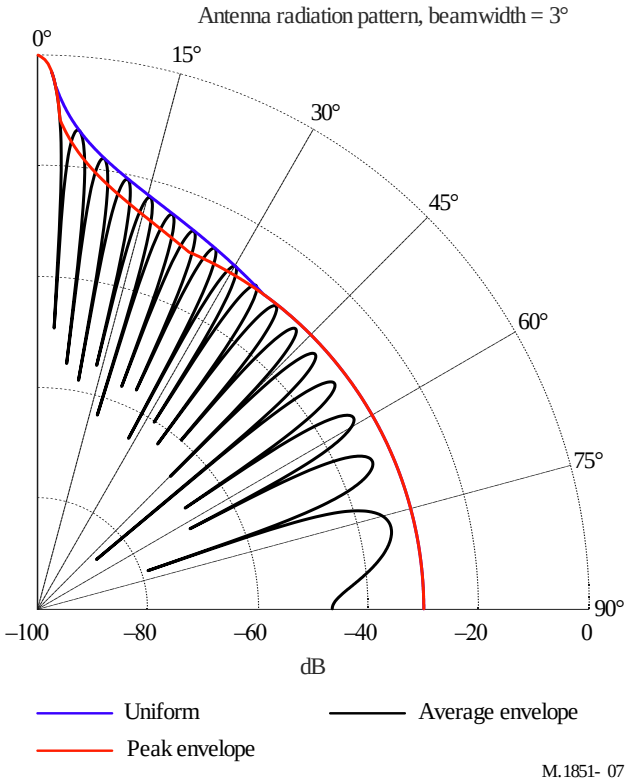


FIGURE 8

**Antenna pattern, peak and average envelope for cosine field distribution**

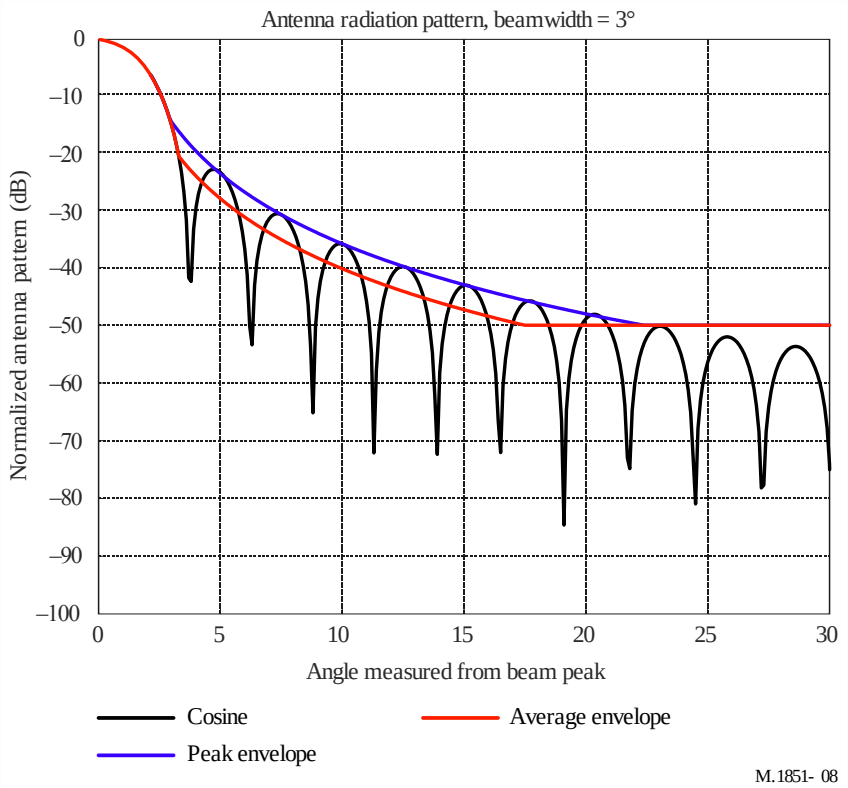

FIGURE 9

**Antenna pattern, peak and average envelope for a cosine-squared distribution**

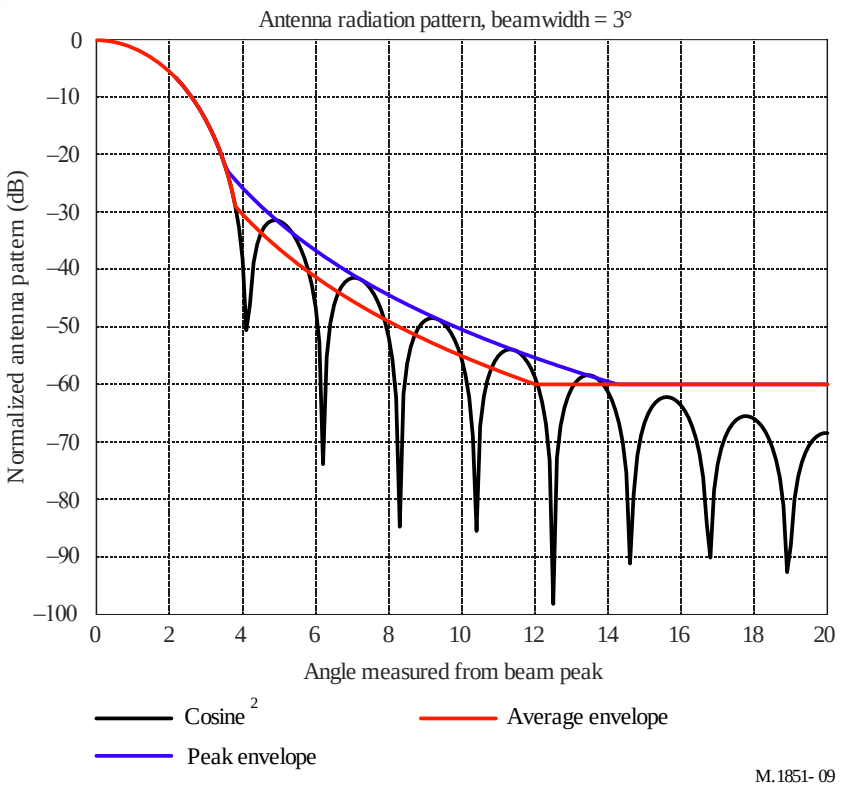


FIGURE 10

**Antenna pattern, peak and average envelope for a cosine-cube distribution**

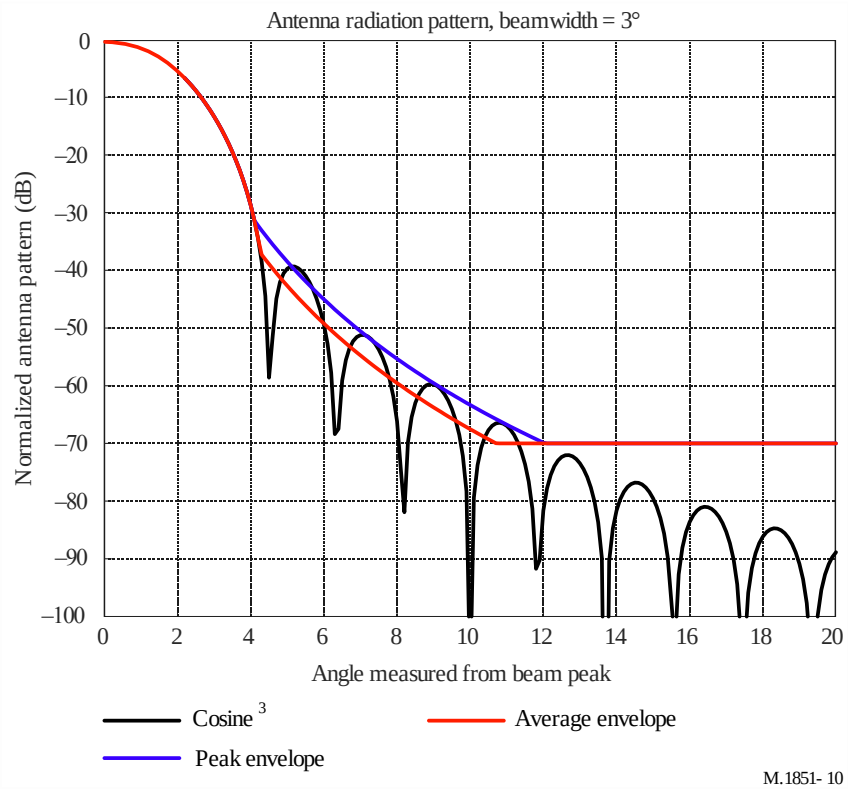

FIGURE 11

**Antenna pattern, peak and average envelope for a cosine-to-the-fourth power distribution**

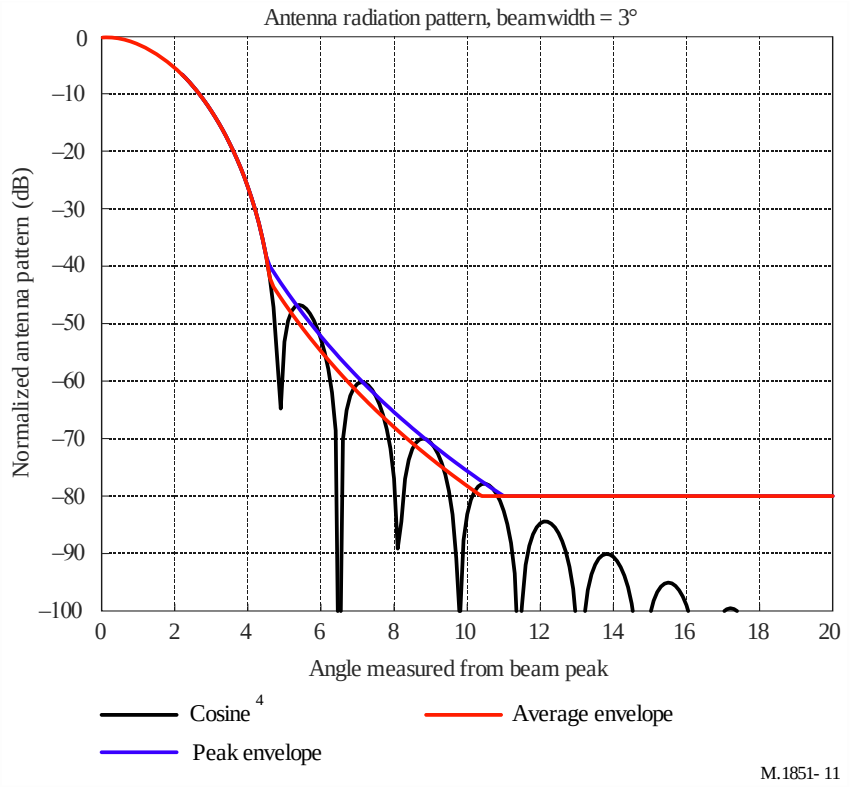


FIGURE 12

**CSC² antenna pattern envelope**

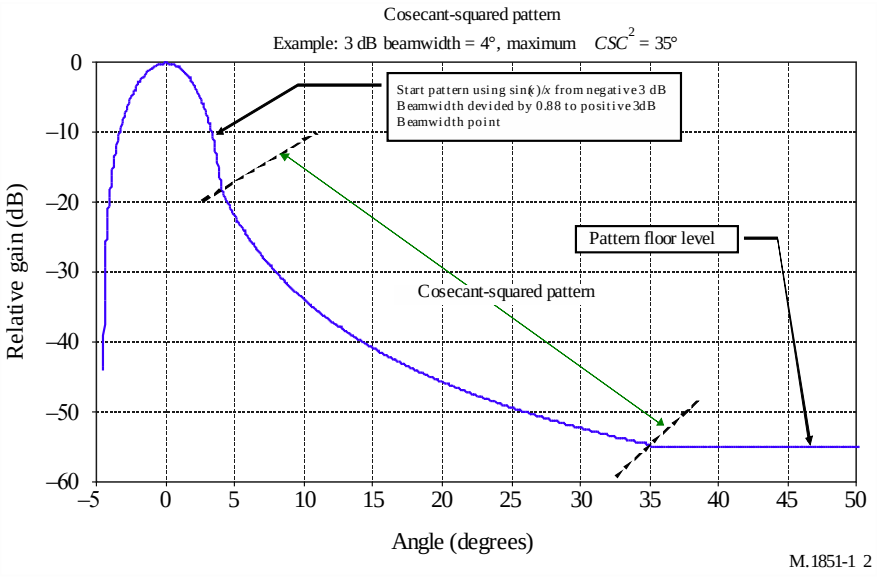


## 3 Antenna pattern selection

A suggestion for how the antenna pattern should be selected is based on information about half-power beamwidth and peak side-lobe level. This is provided in Table 5 given information about half power beamwidth.

TABLE 5

**Pattern approximation selection table**

| Range of first side-lobe level below normalized main lobe peak (dB) | Possible antenna distribution type and cosine raised to power n | Theoretical pattern Equation number | Mask equation number |
|---|---|---|---|
| 13.2 to < 20 | Uniform | (2) | (7) |
| 20 to < 30 | n = 1 | (3) | (8) |
| 30 to < 39 | n = 2 | (4) | (9) |
| 39 to <45 | n = 3 | (5) | (10) |
| >= 45 | n = 4 | (6) | (11) |

## 4 Antenna pattern comparison

One mathematical model for a radiodetermination radar antenna pattern that has been used in interference analysis is given in Recommendation ITU-R M.1652. It includes equations for several patterns as a function of antenna gain. A comparison between the models developed in this Recommendation and Radar-C from Recommendation ITU-R M.1638-0 shows that the pattern in Recommendation ITU-R M.1652 is not optimal. As shown in Fig. 13, the pattern from Recommendation ITU-R M.1652 significantly overestimates the antenna gain off the antenna boresight (0°).

It should also be noted that the equations defined in Recommendation ITU-R F.699 tends to overestimate the sidelobe levels of some radar systems, and it was not developed for radar systems.

FIGURE 13

**Antenna pattern comparison**

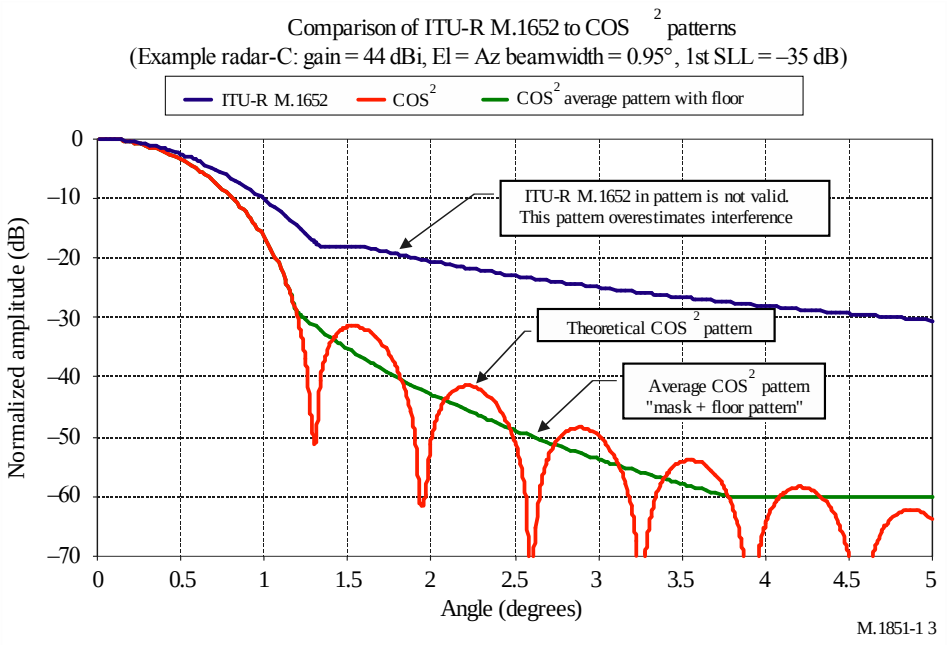


## 5 Approximating three-dimensional (3-D) patterns

Data from the contour plots may be used as simulation analysis tools. The three-dimensional (3-D) antenna pattern can easily be approximated. This is done by multiplying the horizontal and vertical principal plane voltage cuts. To do this, place the vertical principal plane pattern in the centre column of a square matrix, and set all the other elements to zero. Place the horizontal principal plane pattern in the centre row of a square matrix and set all the other elements to zero. Multiply the two matrices together and plot. Note that all patterns must be normalized.

The equation for calculating the 3-D pattern is given by:

$$P_{i,h} = 20 \log\left[\sum_{k=0}^{N} \left| H_{k,i} V_{h,k} \right|\right] \tag{17}$$

where the elevation and azimuth matrices, in units of volts, are defined in equations (18) and (19).

The vertical pattern is given by:

$$\text{Vertical matrix } (V_{h,k}) = \begin{vmatrix} 0 & .... & 0 & El_1 & 0 & .... & 0 \\ 0 & .... & 0 & El_2 & 0 & .... & 0 \\ .... & .... & 0 & El_3 & 0 & .... & .... \\ .... & .... & .... & .... & .... & .... & .... \\ .... & .... & .... & .... & .... & .... & .... \\ 0 & .... & 0 & El_{N-1} & 0 & .... & 0 \\ 0 & .... & 0 & El_N & 0 & .... & 0 \end{vmatrix} \quad (18)$$

The horizontal pattern is given by:

$$\text{Horizontal matrix } (H_{k,i}) = \begin{vmatrix} 0 & .... & .... & .... & .... & 0 \\ .... & .... & .... & .... & .... & .... \\ 0 & 0 & .... & .... & 0 & 0 \\ Az_1 & Az_2 & & & Az_{N-1} & Az_N \\ 0 & 0 & .... & .... & 0 & 0 \\ .... & .... & .... & .... & .... & .... \\ 0 & 0 & .... & .... & .... & 0 \end{vmatrix} \quad (19)$$

Figures 14 and 15 show an example of a 3-D pattern.

FIGURE 14

**Contour Normalized (dB) Pattern**

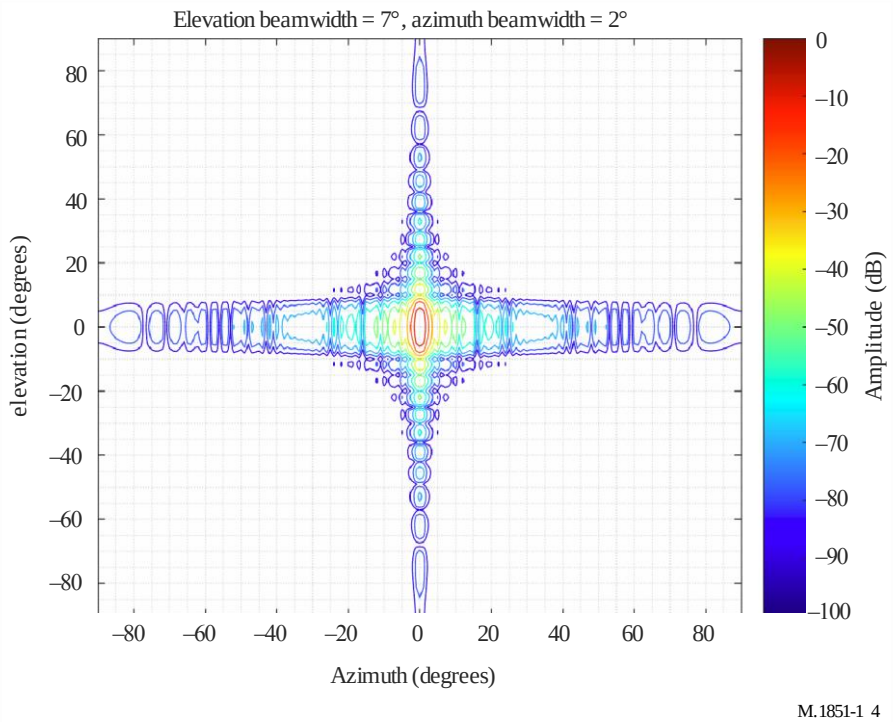

FIGURE 15

**Example of a 3-D relative azimuth and elevation antenna plot, uniform field distribution of a rectangular aperture, attenuation (dB) versus off-axis angle; θ (elevation, degrees) and φ (azimuth, degrees)**

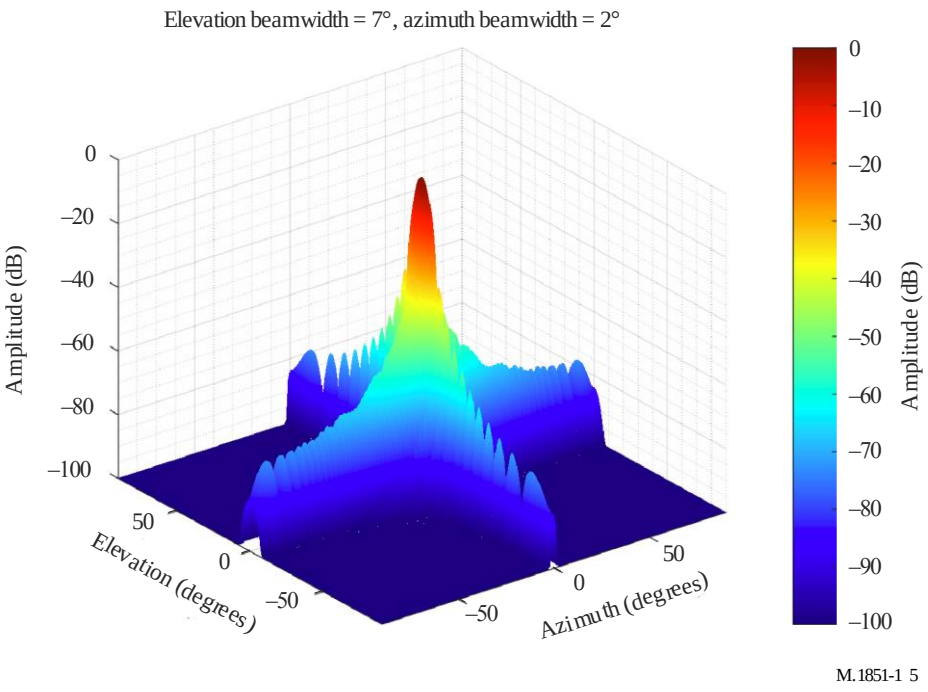


## 6 Measured pattern examples

Figures 16 and 17 show examples of measured radar antenna patterns, in the 9 GHz band. The X axis represents the azimuth angle spanned on more than 360°, and Y axis represents the power level received at each azimuth angle. This power pattern has to be normalized respectively to its maximum or an isotrope antenna to be considered as the antenna pattern or the directivity pattern.

First analysis of such measured antenna patterns indicates that first side lobes appears near −30 dBc with a noticeable slope of side lobes leading to estimate roughly that a $\cos^2$ aperture illumination law was used. A theoretical mask floor at −60 dBc given by $\cos^2$ model would appear in this case a bit too low due to presence of backlobe and rear diffraction lobes in this antenna pattern, then if necessary, encouraging to use real antenna patterns instead of theoretical ones when possible.

FIGURE 16

**Example measured antenna plot**

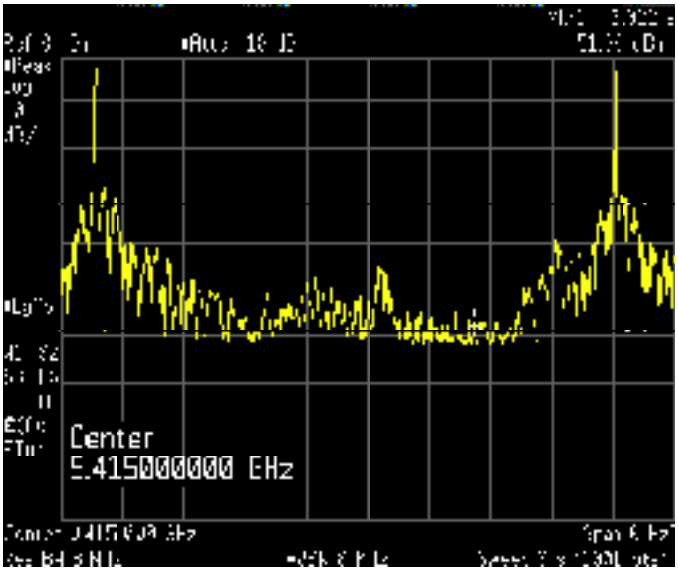


M.1851-1 6

FIGURE 17

**Example measured antenna plot**

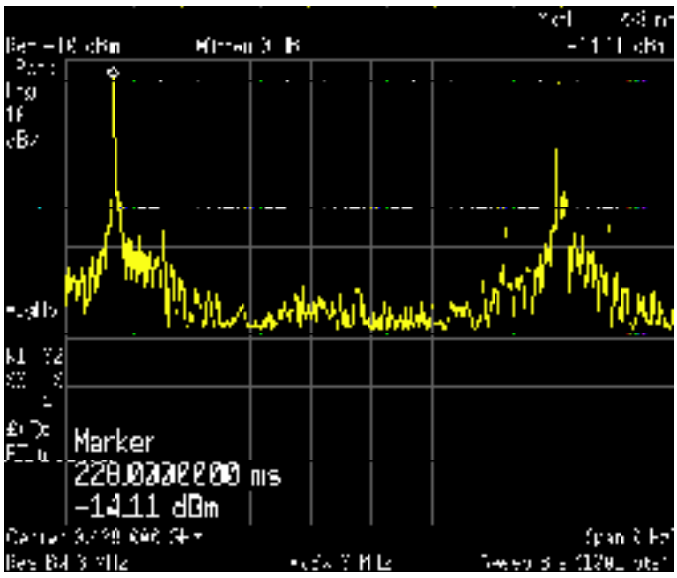


M.1851-1 7

Figures 18 and 19 show two other examples.

FIGURE 18

**Measurement from AN/SPN-6 radar antenna at 3.6 GHz and 38 dBi**

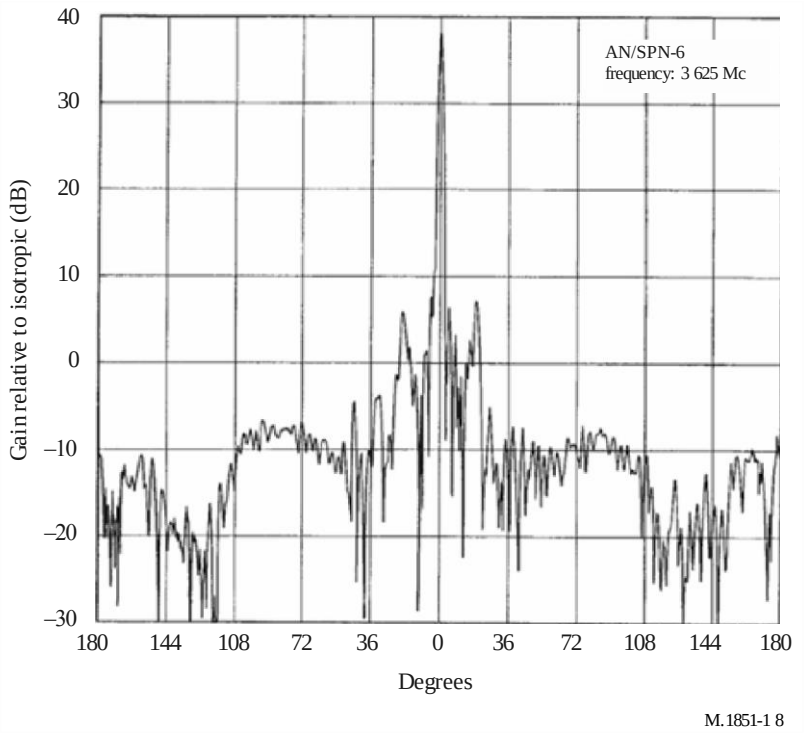


Source: Statistical Characteristics of Gain and Mutual Gain of Radar Antennas, Project No. SF 010 204, Task 5727, Department of the Navy 15 September, 1963

FIGURE 19

**Doppler radar antenna pattern from meteorological radar with 25 dB 1st sidelobe and 60 dB front-to-back ratio**

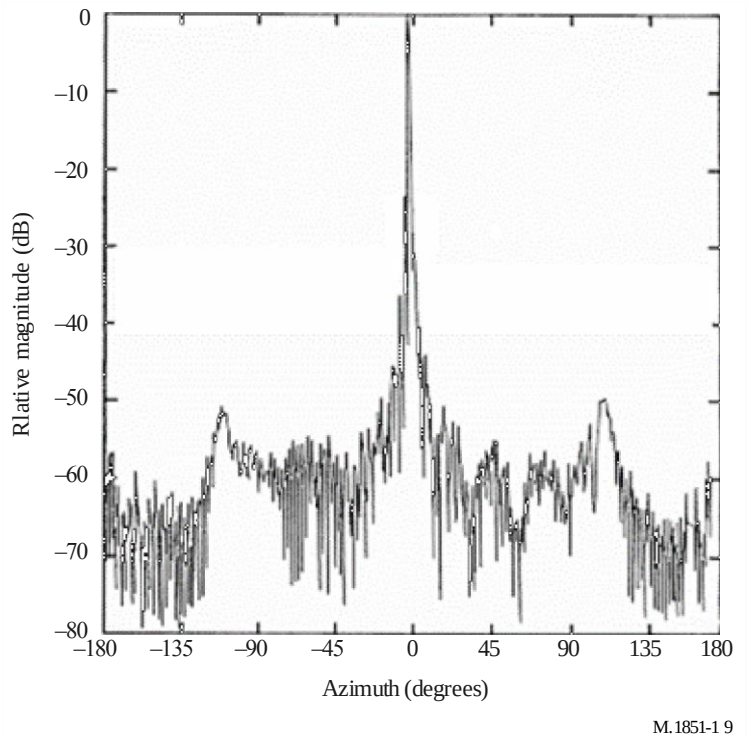

Source: USA Federal Meteorological Handbook No. 11, December 2005 Part B, FCM-H11B-2005

## 7 Patterns for phased array antennas

The following equation could be used in the calculations for uniform linear array antenna normalized pattern:

$$g(\theta) = f(\theta).\frac{1}{N}\left|AF(\theta)\right|^2 \tag{20}$$

where

*g*: uniform linear array antenna normalized gain pattern

*f*: Elementary radiating elements normalized gain pattern inserted in the uniform linear array antenna

*N*: number of elementary radiating elements

*AF*: uniform linear array antenna factor; Ψ (radians):

$$AF(\theta) = \frac{\sin\left(\frac{N\Psi}{2}\right)}{\sin\left(\frac{\Psi}{2}\right)} \tag{21}$$

with

$$\Psi = 2\pi(d/\lambda)(\sin(\theta) - \sin(\omega)) \tag{22}$$

where

*d*: uniform elementary radiating element regular interspace

λ: wavelength at the considered frequency

ω: electronicaly beam steering angle

θ: off-axis angle.

FIGURE 20

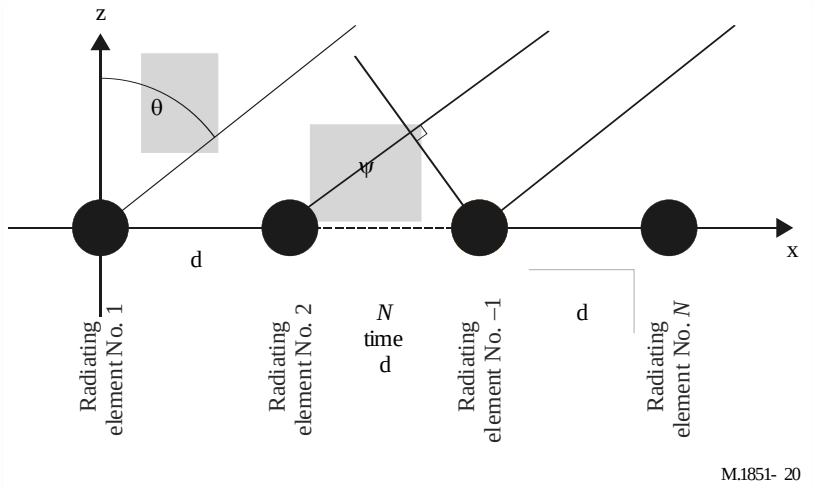


The specific nature of phased array antennas allows to steer electronically the mainlobe of the antenna pattern in a ±90° range from the mechanical antenna boresight. At large scan ω angles specific sidelobes effects in the antenna patterns should be taken into account as mainlobe significant

enlargement and desymmetrization (see Fig. 22). In fact the main lobe maximum value decreases as cos(ω) and further as the elementary radiating element pattern in the array. This result is a widened mainbeam, max gain losses, and consequently far sidelobes increase. For value of ω between ±60° and ±90° range from the mechanical antenna boresight the resulting pattern is so perturbed that it is no more usable (see Fig. 24). The practical values of ω are between 0° and ±60° range from the mechanical antenna boresight. Furthermore, if the array lattice is bigger than λ/2 among the elementary radiating elements in the array, grating lobes of the mainlobe could appear for ω even less than ±60° range from the mechanical antenna boresight (see Fig. 23). And even if the array lattice is λ/2 among the elementary radiating elements in the array, sidelobes of the grating lobes of the mainlobe, situated at −90° and +90° from the mechanical antenna boresight, disturb the array pattern (see Fig. 24).

FIGURE 21

**Theoretical radiating pattern of an Uniform Linear Array of 30 radiating elements with a λ/2 lattice (blue curve) with a cosine$^2$ radiating pattern (red curve) steered at boresight**

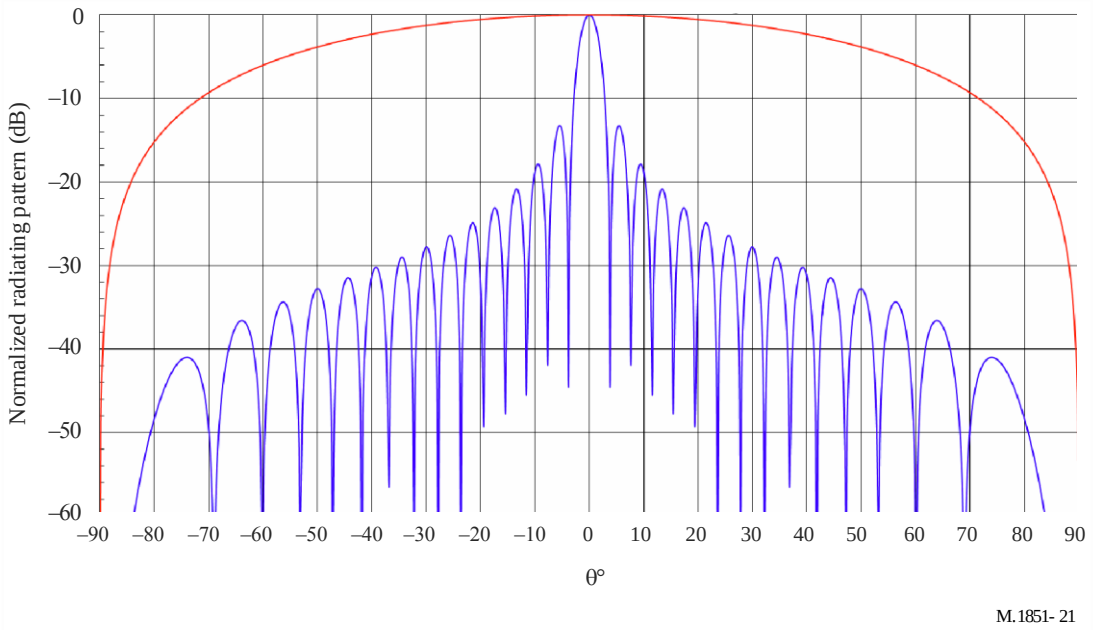

FIGURE 22

**Theoretical radiating pattern of an Uniform Linear Array of 30 radiating elements with a λ/2 lattice (blue curve) with a cosine² radiating pattern (red curve) steered at 60°**

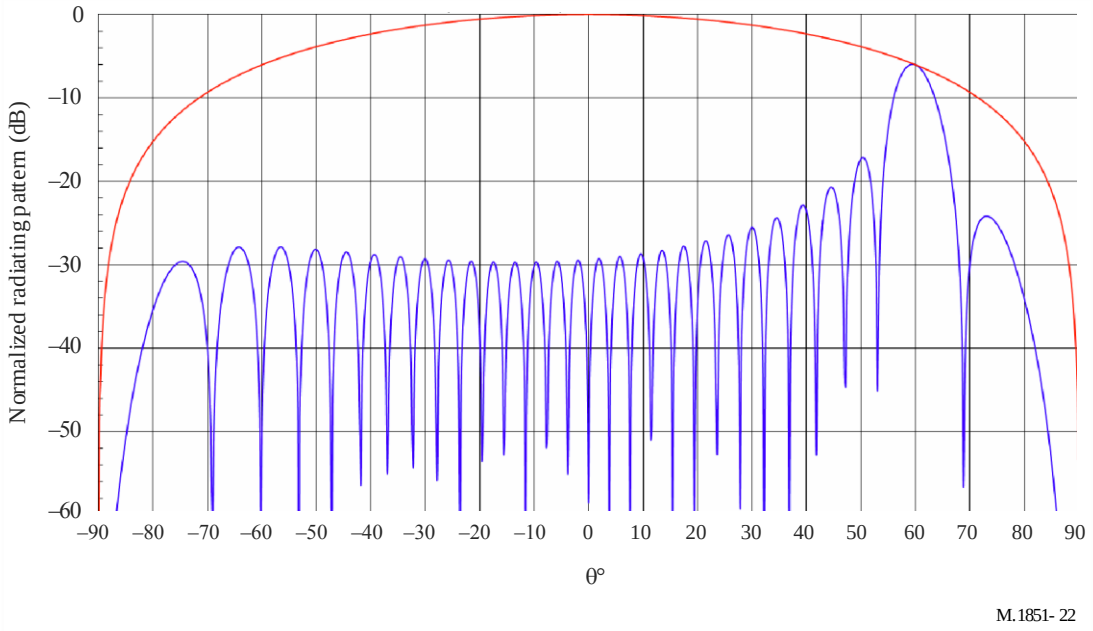


FIGURE 23

**Theoretical radiating pattern of an Uniform Linear Array of 30 radiating elements with a 0.6λ lattice (blue curve) with a cosine² radiating pattern (red curve) steered at 45°**

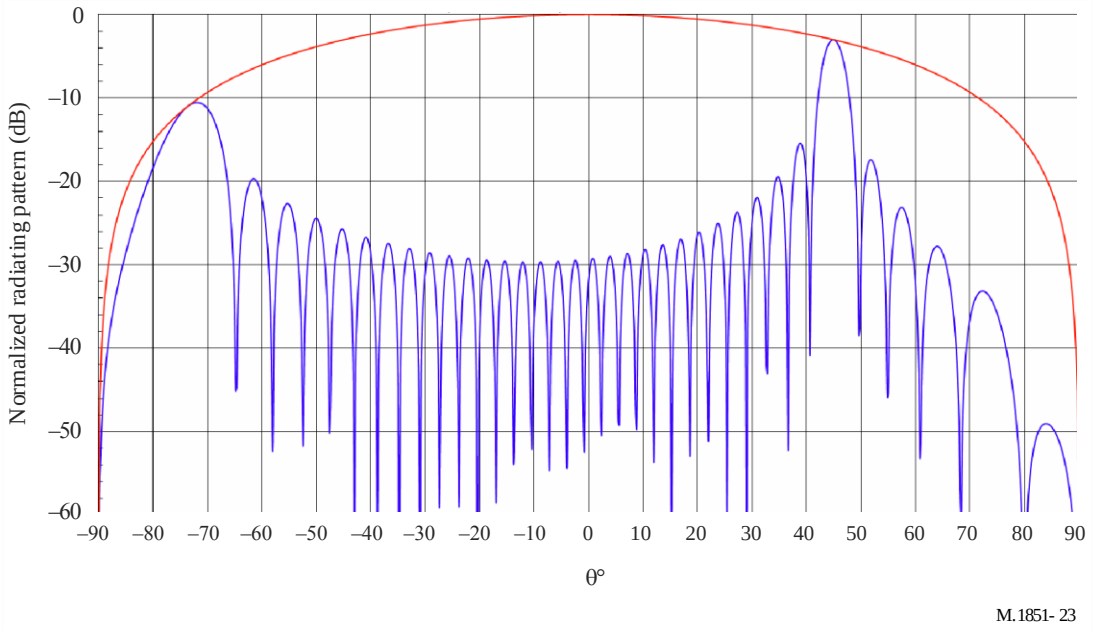

FIGURE 24

**Theoretical radiating pattern of an Uniform Linear Array of 30 radiating elements with a λ/2 lattice (blue curve) with a cosine$^2$ radiating pattern (red curve) steered at 80°**